PERGAMON

International Journal of Solids and Structures 38 (2001) 1–28

INTERNATIONAL JOURNAL OF SOLIDS and STRUCTURES

www.elsevier.com/locate/ijsolstr

Singular full-field stresses in composite laminates with open holes

E.V. Iarve *, N.J. Pagano

Non-metallic Materials Division, Air Force Research Laboratory, Wright-Patterson AFB, Ohio, USA

Received 17 July 1998; in revised form 6 January 1999

Abstract

A method of the superposition of a hybrid and displacement approximation was developed to provide the accurate stress fields in a multilayered composite laminate, including the singular neighborhood of the ply interface and the hole edge. Asymptotic analysis was used to derive the hybrid stress functions. The displacement approximation is based on the polynomial B-spline functions. The method provides the determination of the coefficient of the singular term along with convergent stress components including the singular regions. Reissner's variational principle was employed. Simple $[45/-45]_s$ and quasi-isotropic IM7/5250 $[45/90/-45/0]_s$ laminates were analyzed. Uniaxial loading and residual stress calculation (quasi-isotropic laminate) were considered. A convergence study showed that accurate values of the coefficient of the singular term of the asymptotic stress expansion could be obtained with coarse out-of-plane and in-plane subdivisions. The interaction between the singular terms on the neighboring interfaces was found to be important for the convergence with coarse subdivisions. Converged transverse interlaminar stress components as a function of the distance from the hole edge, were shown for all examples.

Keywords: Composite; Laminate; Open hole; Singularity; Asymptotic solution; B-splines; Hybrid approximation; Reissner's variational principle

1. Introduction

Development of the methods, for an efficient stress analysis of the composite structures containing curvilinear edges such as cutouts, etc., is of significant practical interest. Ply level models of the laminated composites, according to which a lamina is modeled as a homogeneous orthotropic material, result in a singular stress behavior in the vicinity of the ply interface and laminate edge. The present article deals with a three-dimensional elasticity analysis in the presence of the singular stresses and focuses on representing the stress field by using a superposition of the asymptotic solution and polynomial spline approximation.

A valuable experience was gained due to considerable effort devoted to the solution of the straight free edge problems. A hybrid approximation, based on an assumed equilibrium stress field was proposed by

* Corresponding author. Address: University of Dayton, Research Institute, 300 College Park, Dayton, OH 45469-0168, USA. Fax: +1-513-258-8075.

E-mail address: iarveev@ml.wpafb.af.mil (E.V. Iarve).

0020-7683/00/$ - see front matter
PII: S0020-7683(00)00007-X

Pagano (1978a,b) using Reissner's variational principle. Without including the precise singular stress terms, highly accurate stress predictions for various laminates were demonstrated. The singular term of the asymptotic solution for the composite wedge near the ply interface and the wedge edge was obtained by Mikhailov (1979). The power of singularity was determined as a function of ply anisotropy and wedge angle. Independently, Wang and Choi (1982) constructed an infinite series elasticity solution for the same problem based on Lekhnitskii's complex variable stress function. The singular stress term was precisely determined. A polynomial particular solution was added to satisfy the axial loading condition. Determination of the unknown multiplicative factors in the homogeneous solution, including the coefficient of the singular term, was accomplished by the boundary collocation method. The results for a $[\pm 45]_s$ laminate were shown to converge using 30 eigenfunctions of the homogeneous solution. A hybrid finite element formulation (Tong et al., 1973) based on this solution was developed by Wang and Yuan (1983).

Folias (1992) and Wang and Lu (1993) considered stresses in laminated composites at the interface and the open hole edge. They showed that the zeroth order term of the asymptotic expansion of the three-dimensional elasticity equations in terms of the parameter $\lambda = h/D$ (ply thickness/hole diameter) yields a two-dimensional elasticity problem. Thus, the singular stress term at the ply interface and the curvilinear edge is the same as that for the straight edge, provided the ply orientations are the same, relative to the tangent to the curved edge. However, extending these results to obtain a full-field solution is not trivial. The critical difference is that, the analytically obtained eigenfunctions of the asymptotic two-dimensional field do not satisfy the three-dimensional equations in any finite volume. Thus, no exact homogeneous solution is constructed in a finite volume surrounding the intersection of the hole edge and the orthotropic ply interface. It should be noted that an impressive convergence of the hybrid singular finite element formulation was demonstrated (Tong et al., 1973; Wang, 1983) for problems, where the assumed stress functions in relatively large singular elements actually provided elasticity solutions over the entire element. An assumed, displacement based finite element formulation including the singular asymptotic term was developed by Wang and Lu (1993), and the stress intensity factor for a ± 45 laminate was obtained as a function of the circumferential coordinate. However, insufficient information was given to allow one to comment on the rate of convergence. It was noted that the asymptotic solution was included in the formulation only over a small region near the free edge of the cutout.

Iarve (1996) developed a B-spline based approximate three-dimensional solution for the multilayered composite laminates containing open holes. It was also shown that a two-dimensional problem (with θ as a parameter) identical to the one obtained asymptotically in Folias (1992), and Wang and Lu (1993) follows from the three-dimensional formulation assuming vanishing of the spatial derivatives in the circumferential (θ) direction. The numerically obtained stress distributions near the hole edge were compared to the stresses given by the singular term of the asymptotic solution. At the singularity, the polynomial spline approximation does not capture the directional non-uniqueness of the singular stress functions, Pagano and Kaw (1995), and resulted in an interfacial traction discontinuity. However, it was observed that the singular term of the asymptotic solution with appropriate coefficient and constant additive terms matched the full-field spline solution at approximately one half-ply thickness from the singular point. The surprisingly large area of agreement suggests that superposition of the singular term and the polynomial approximation, may be utilized for the determination of the stress intensity factor.

Morley (1969, 1970) pioneered the idea of superposition of the analytical and finite element solution in the problems with local field singularities. His approach is based on the Rayleigh–Ritz method where the polynomial displacement approximation is enriched through the entire domain, by the local analytical (asymptotic) solution minus its finite element approximation. The analytical solution must satisfy the field equations and the homogeneous boundary conditions of the problem. The finite element approximation is obtained under the boundary conditions generated by the analytical solution with unit stress intensity factor. For sufficiently fine meshes, the analytical solution and its approximation will differ only in the vicinity of the singular point. The scaling factors, which are the coefficients of the additional terms used for

enrichment of the finite element basis, are obtained through a variational procedure. Yamamoto and Tokuda (1973) applied this method to crack stress intensity factor determination, using a multiple term asymptotic expansion for the analytical solution. They used a boundary collocation method to obtain the coefficients of the terms containing analytical solutions.

For the curvilinear edge singularities considered in the present article, the analytical solution in the finite domain near the singularity is unknown. The asymptotic solution obtained in (Folias, 1992; Wang, 1993; Iarve, 1996) is a two-dimensional solution in nature and cannot be used directly in the approach described in Morley (1969, 1970) and Yamamoto and Tokuda (1973). It should be mentioned that Yamamoto and Sumi (1978) considered an axisymmetric problem of a twisted round isotropic bar with an annular crack. The asymptotic solution, which was used as the basis for the analytical solution near the crack tip, was equivalent to a local plane strain solution which did not satisfy the axisymmetric equilibrium equations throughout the domain. The asymptotic solution for the round isotropic bar problem, which was reduced to a single unknown function – the circumferential displacement component – was augmented by a higher-order term added to the asymptotic solution to satisfy the equilibrium equations. However, in a general orthotropic case, these complementary terms are not obvious and have not been reported in the literature.

The present article extends the superposition approach to problems where no analytical solutions in the finite domain are known. The model developed is based on Reissner's variational principle and is intended to reflect the singularities, which arise at each interface at the boundary of the hole. The hybrid approximation functions to be developed, have the following characteristics:

(1) They include the asymptotic solution thus representing the directional non-uniqueness of the solution. It is only in this manner that one can embed the proper singular field. The fact that the asymptotic solution results from the three-dimensional problem by truncating the spatial derivatives in the circumferential direction (Iarve, 1996) will be used to construct hybrid stress functions.

(2) Two independent (B-spline) displacement functions are considered: One is related to the regular and the other to the singular portion of the stress field. It is undesirable to use the asymptotic displacement functions in the displacement approximation because, the calculation of their derivatives in the circumferential direction, required in the variational formulation, is only possible numerically. It is assumed that the displacements related to the singular stresses will also be approximated with splines. Thus, the approximations of stresses and displacements are made independently.

Examples to demonstrate the convergence with respect to meshing parameters will be considered.

2. Problem statement

Consider a rectangular N-layer laminate built of orthotropic layers with length L in the x-direction, width A in the y-direction, and thickness H. Individual ply thicknesses are $h_p = z^{(p)} - z^{(p-1)}$, where $z = z^{(p)}$ and $z = z^{(p-1)}$ are upper and lower surfaces of the p-th ply, respectively. The origin of the x, y, z coordinate system is in the lower left corner of the plate, as shown in Fig. 1. A circular opening of diameter D with the center at $x = x_c$ and $y = y_c$ is considered. Uniaxial loading is applied via displacement boundary conditions at the lateral sides ($x = 0, L$):

$$-u_x(0,y,z) = u_x(L,y,z) = u_0, \quad u_y(0,y,z) = u_y(L,y,z) = 0. \tag{1}$$

The transverse displacement is not constrained aside from a rigid body constant, and the respective traction $T_z = 0$ is prescribed. The edge of the opening is a part of the traction prescribed loading boundary S_T, so that

$$\sigma_{ij} n_j = T_i(x_i), \quad x_i \in S_T,$$

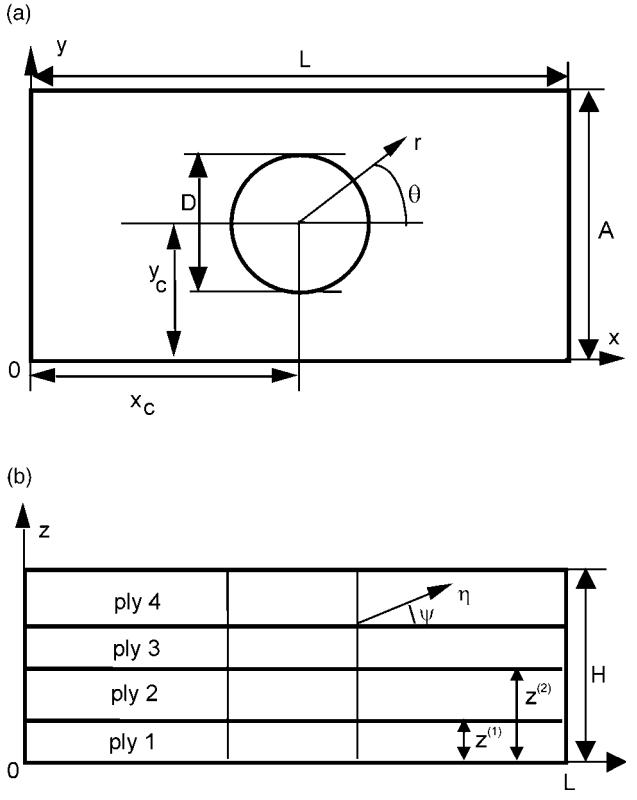

Fig. 1. Plate with the hole and coordinate systems.

where tractions T_i are known. Indices $i, j = 1, 2, 3$ correspond to the directions x, y, z, respectively. The lateral edges $y = 0, A$ and the surfaces $z = 0, H$ also belong to S_T. The constitutive relations in each ply are as follows:

$$\sigma_{ij} = C^p_{ijkl}(\varepsilon_{kl} - \alpha^p_{kl}\Delta T),$$

where C^p_{ijkl} and α^p_{kl} are elastic moduli and thermal expansion coefficients of the pth orthotropic ply, and ΔT is the temperature change. A cylindrical coordinate system r, θ, z with the origin at $(x_c, y_c, 0)$ is introduced

$$x = r\cos\theta + x_c, \qquad y = r\sin\theta + y_c, \qquad z = z.$$

According to the asymptotic analysis performed in the earlier articles (Folias, 1992; Wang, 1993; Iarve, 1996), the stresses in the vicinity of the hole edge and the interface between the p and $p+1$ plies are thought to be of the form:

$$\sigma_{ij} = \sum_{\lambda} K_s(\theta)\eta^{\lambda-1} f_{ij}(\psi, \theta) + \text{bounded function}.$$

The first terms represent the unbounded ($0 < \mathrm{Re}(\lambda) < 1$) singular stress terms, where η and ψ are local coordinates introduced in the cross-section $\theta = \text{const}$ (Fig. 1b) according to equation

$$\eta\cos\psi = r - D/2, \qquad \eta\sin\psi = z - z^{(p)}. \tag{2}$$

The asymptotic solution is normalized similar to (Wang, 1993) so that

$$K_p(\theta) = \lim_{\eta\to 0}[\eta^{1-\lambda}\sigma_{zz}(D/2 + \eta\cos\psi, z^{(p)}, \theta)].$$

The singular term,

$$a_{ij} = \eta^{\lambda-1} f_{ij}(\psi, \theta)$$

is a solution of the asymptotically derived two-dimensional problem and satisfies neither the three-dimensional equilibrium nor the compatibility equations in any finite volume around the curved boundary. However, it does satisfy the traction-free boundary conditions on the hole edge as well as the interface continuity conditions in the limit $\eta \to 0$. We shall consider one singular term at each angular location, at each interface at the open hole edge, with the extension to an arbitrary number of terms at the same singular point being straightforward. The displacement components and the bounded portion of the stresses will be approximated by using cubic spline functions, and Reissner's variational principle will be applied in order to obtain $K_p(\theta)$ and the unknown spline approximation coefficients. The asymptotic solution near the orthotropic ply interface and the hole edge will be considered next.

3. Asymptotic solution

Consider a region around the hole edge and the interface between plies p and $p+1$. A local coordinate system η, ψ is introduced in the radial cross section $\theta = \text{const}$ according to Eq. (2). In this coordinate system $0 \leqslant \psi \leqslant \pi/2$ in the upper ply and $-\pi/2 \leqslant \psi \leqslant 0$ in the lower one.

For an arbitrary function F,

$$\frac{\partial F}{\partial r} = \Lambda_t F, \quad \frac{\partial F}{\partial z} = \Lambda_n F,$$

where

$$\Lambda_t F = \frac{\partial F}{\partial \eta}\cos\psi - \frac{1}{\eta}\frac{\partial F}{\partial \psi}\sin\psi, \qquad \Lambda_n F = \frac{\partial F}{\partial \eta}\sin\psi + \frac{1}{\eta}\frac{\partial F}{\partial \psi}\cos\psi.$$

In Cartesian coordinates, the derivatives can be calculated as

$$\begin{aligned} \frac{\partial F}{\partial x} &= (\cos\theta)\Lambda_t F - \frac{\sin\theta}{D/2 + \eta\cos\psi}\frac{\partial F}{\partial \theta}, \\ \frac{\partial F}{\partial y} &= (\sin\theta)\Lambda_t F + \frac{\cos\theta}{D/2 + \eta\cos\psi}\frac{\partial F}{\partial \theta}. \end{aligned} \tag{3}$$

If $\eta \to 0$, then the first terms in the right-hand side of both Eqs. (3) are of the order F/η and the second terms are of the order F. Thus, for small η, the expressions for derivatives (3) are truncated by retaining only the first terms, so that

$$\begin{aligned} \frac{\partial F}{\partial x} &\cong \left(\frac{\partial F}{\partial x}\right)_\theta = \frac{\partial F}{\partial r}\cos\theta = \Lambda_t F\cos\theta, \\ \frac{\partial F}{\partial y} &\cong \left(\frac{\partial F}{\partial y}\right)_\theta = \frac{\partial F}{\partial r}\sin\theta = \Lambda_t F\sin\theta, \quad \eta \to 0, \\ \left(\frac{\partial F}{\partial z}\right)_\theta &= \frac{\partial F}{\partial z} = \Lambda_n F, \end{aligned} \tag{4}$$

where the notation $(\ )_\theta$ implies truncation by deletion of the θ derivative. Although these equations are exact in the limit $\eta \to 0$ only, we shall use these derivatives through a finite volume to construct the hybrid approximation. Under these assumptions, the Navier equations of a given ply will simplify to

$$(\mathbf{A}\Lambda_t\Lambda_t + \mathbf{B}\Lambda_n\Lambda_t + \mathbf{C}\Lambda_n\Lambda_n)\begin{bmatrix} u_x \\ u_y \\ u_z \end{bmatrix} = 0,$$

where the 3×3 matrices **A**, **B**, **C** are given in the appendix and depend upon the elastic moduli and θ. Note that the thermal expansion coefficients do not enter these equations due to the assumption of a uniform temperature change. The solution of the Navier equations can be found in the form:

$$u_i = \sum_{\lambda} v_i^p(\eta^\lambda, \psi, \theta) + U_i^p(\eta, \psi, \theta),$$

where $U_i^p(\eta, \psi, \theta)$ is a particular solution and $\sum_\lambda v_i^p(\eta^\lambda, \psi, \theta)$ is the homogeneous solution.

Non-homogeneous boundary conditions resulting from non-zero prescribed tractions or thermal mismatch can be satisfied with a piecewise polynomial particular solution of appropriate order, provided that the prescribed tractions are smooth and bounded within the ply though perhaps discontinuous at the interfaces. The thermal expansion strains are not present for the homogeneous solution and will be determined in a particular solution. We shall be interested in the homogeneous solutions v_i^p, which have essentially non-polynomial format, and the respective tractions satisfying homogeneous boundary conditions. The homogeneous solution of the displacement field can be written as (Iarve, 1996)

$$v_i^p = \eta^\lambda \sum_{k=1}^{6} \gamma_k d_{ki}^p (\sin\psi + \mu_k^p \cos\psi)^\lambda,$$

where the superscript p refers to the ply number. It will be understood that coefficients μ_k and vectors $\{d_{ki}\}$ are constants for each ply; therefore, the superscript is subsequently omitted, unless needed for clarity. The stresses from the homogeneous solution are

$$\sigma_{ij}^p = C_{ijkl}^p \left(\left(\frac{\partial v_k^p}{\partial x_l} \right)_\theta + \left(\frac{\partial v_l^p}{\partial x_k} \right)_\theta \right),$$

where the truncated derivatives are calculated by using expressions (4). The expression for the stresses may be written in the form,

$$\sigma_{ij}^p = \lambda \eta^{\lambda-1} \sum_{k=1}^{6} \gamma_k c_{ij}^{k,p} (\sin\psi + \mu_k \cos\psi)^{\lambda-1}.$$

Coefficients $c_{ij}^{k,p}$, defined in Iarve (1996), depend upon elastic moduli of the pth ply. It was taken into account that the following relationship applies for the differential operators:

$$\Lambda_t v_i^p = \lambda \eta^{\lambda-1} \sum_{k=1}^{6} \gamma_k d_{ki} \mu_k (\sin\psi + \mu_k \cos\psi)^{\lambda-1},$$

$$\Lambda_n v_i^p = \lambda \eta^{\lambda-1} \sum_{k=1}^{6} \gamma_k d_{ki} (\sin\psi + \mu_k \cos\psi)^{\lambda-1},$$

which leads to the following characteristic equation for obtaining μ_k:

$$\det[\mathbf{A}\mu_k^2 + \mathbf{B}\mu_k + \mathbf{C}] = 0,$$

where $\{d_{ki}\}$ are eigenvectors of the characteristic matrix:

$$[\mathbf{A}\mu_k^2 + \mathbf{B}\mu_k + \mathbf{C}]\begin{bmatrix} d_{k1} \\ d_{k2} \\ d_{k3} \end{bmatrix} = 0.$$

The power λ and coefficients γ_k are defined from the boundary conditions of displacement and traction continuity at the interface between plies p and $p+1$

$$\psi = 0: \; v_i^p(\eta,0,\theta) = v_i^{p+1}(\eta,0,\theta), \quad \sigma_{zi}^p(\eta,0,\theta) = \sigma_{zi}^{p+1}(\eta,0,\theta), \qquad i = x,y,z,$$

and the traction-free boundary conditions imposed at the hole edge:

$$\sigma_{ri}^{p+1}\left(\eta,\frac{\pi}{2},\theta\right) = 0, \quad i = r,\theta,z,$$

$$\sigma_{ri}^{p}\left(\eta,-\frac{\pi}{2},\theta\right) = 0, \quad i = r,\theta,z.$$

Non-trivial solutions of the homogeneous boundary value problem exist for discrete values of λ only. Coefficients γ_k are obtained to satisfy the interfacial and hole edge boundary conditions.

We shall be interested in the solutions when $0 < \mathrm{Re}(\lambda) < 1$. These terms provide unbounded stresses, which dominate the solution for small η. In the context of the present work, laminates with more than one interface will be considered, and the singular asymptotic terms will be used at each interface. For convenience, we will introduce an analytical continuation of the asymptotic displacements into all plies of the laminate. Thus, we extend the definition of the displacement vector v_i^p and stress components a_{ij}^p for the asymptotic solution associated with interface $z^{(p)}$ between plies p and $p+1$ depending upon the properties of the ply in which ψ is located [1]

$$v_i^p = \begin{cases} \eta^\lambda \sum_{k=1}^{6} \gamma_k d_{ki}^{p+1} (\sin\psi + \mu_k^{p+1}\cos\psi)^\lambda, & \psi > 0, \\ \eta^\lambda \sum_{k=1}^{6} \gamma_k d_{ki}^{p} (\sin\psi + \mu_k^{p}\cos\psi)^\lambda, & \psi \leqslant 0, \end{cases} \tag{5}$$

and

$$a_{ij}^p = \begin{cases} \lambda\eta^{\lambda-1} \sum_{k=1}^{6} \gamma_k c_{ji}^{k,q} (\sin\psi + \mu_k^{p+1}\cos\psi)^{\lambda-1}, & \psi > 0, \; q = p+1,\ldots,N \\ \lambda\eta^{\lambda-1} \sum_{k=1}^{6} \gamma_k c_{ji}^{k,q} (\sin\psi + \mu_k^{p}\cos\psi)^{\lambda-1}, & \psi \leqslant 0, \; q = 1,\ldots,p \end{cases} \qquad z^{(q-1)} \leqslant \eta\sin\psi + z^{(p)} < z^{(q)}. \tag{6}$$

These functions are defined through the entire laminate thickness. The stresses a_{ij}^p are calculated from strains defined by the truncated derivatives of displacements v_i^p using the elastic moduli of that ply where the stresses are evaluated. The asymptotic solution obtained between plies p and $p+1$ will provide a non-zero stress contribution in a large area surrounding the singular point due to the weak character of the singularity $\lambda - 1 \approx -0.05$ (Mikhailov, 1979; Wang, 1982; Folias, 1992; Wang, 1993; Iarve, 1996) between similar orthotropic layers with different fiber orientations.

4. Variational formulation

Displacement components are represented as

$$u_i = u_i^s + u_i^r, \tag{7}$$

[1] Note that we have refrained from using indices on the variables η an ψ since they always emanate from the singular point at $z = z^{(p)}$. Also, λ has been given no subscript as we only use the lowest possible value at $z = z^{(p)}$.

where the displacements u_i satisfy boundary conditions (1). The term u_i^s is associated with singular stress components and the second term u_i^r with bounded stress components. The stresses will be assumed as

$$\sigma_{ij} = \sigma_{ij}^{\mathrm{hyb}} + \sigma_{ij}^r, \tag{8}$$

The stresses $\sigma_{ij}^{\mathrm{hyb}}$ and displacements u_i^s are independently assumed. The stresses σ_{ij}^r and displacements u_i^r are related as follows:

$$\sigma_{ij}^r = C_{ijkl}^q(u_{(k,l)}^r - \alpha_{kl}^q \Delta T), \tag{9}$$

where C_{ijkl}^q and α_{kl}^q are elastic modulii and thermal expansion coefficients of the qth orthotropic ply, ΔT is the temperature change, and

$$u_{(i,j)} = \frac{1}{2}\left(\frac{\partial u_i}{\partial x_j} + \frac{\partial u_j}{\partial x_i}\right). \tag{10}$$

Reissner's variational principle $\delta R = 0$ is employed, where the functional R is given by equation

$$R = \int\int\int_V (-\Phi(\sigma_{ij}, \Delta T) + \sigma_{ij} u_{(i,j)})\,\mathrm{d}V - \int\int_{S_T} T_i u_i\,\mathrm{d}s, \tag{11}$$

$$\Phi(\sigma_{ij}, \Delta T) = \tfrac{1}{2} S_{ijkl}^q \sigma_{ij}\sigma_{kl} + \sigma_{ij}\alpha_{ij}^q \Delta T, \qquad \left\{S_{ijkl}^q\right\} = \left\{C_{ijkl}^q\right\}^{-1}.$$

Substituting Eqs. (7) and (8) into Eq. (11), one obtains after algebraic manipulations and use of Betti's law:

$$R = \int\int\int_V \left[-\Phi\left(\sigma_{ij}^{\mathrm{hyb}}, 0\right) + \sigma_{ij}^{\mathrm{hyb}} u_{(i,j)}^s - W(u_{(i,j)}^s, 0)\right]\mathrm{d}V + \int\int\int_V W(u_{(i,j)}^r + u_{(i,j)}^s, \Delta T)\,\mathrm{d}V - \int\int_{S_T} T_i(u_i^r + u_i^s)\,\mathrm{d}s, \tag{12}$$

where

$$W(\varepsilon_{ij}, \Delta T) = \tfrac{1}{2} C_{ijkl}^q(\varepsilon_{ij} - \alpha_{ij}^q \Delta T)(\varepsilon_{kl} - \alpha_{kl}^q \Delta T).$$

The goal of the formulation is to treat problems when the external tractions T_i and/or the interfacial tractions can not be approximated pointwise by using the same shape functions as the displacement components or their derivatives. Let the functions X_m be the basis functions for approximation of the displacements u_i^r and the functions Y_m, those for the displacements u_i^s. Then, the following systems of equations will be obtained by taking the variations with respect to the unknown approximation coefficients:

$$\int\int\int_V \left[C_{ijkl}^q(u_{(k,l)}^r - \alpha_{kl}^q \Delta T) + C_{ijkl}^q u_{(k,l)}^s\right] X_{m,j}\,\mathrm{d}V = \int\int_{S_T} T_i X_m\,\mathrm{d}S,$$

$$\int\int\int_V \left[C_{ijkl}^q(u_{(k,l)}^r - \alpha_{kl}^q \Delta T) + \sigma_{ij}^{\mathrm{hyb}}\right] Y_{m,j}\,\mathrm{d}V = \int\int_{S_T} T_i Y_m\,\mathrm{d}S.$$

Both sets of basis functions X_m and Y_m in the present context are of the same piecewise polynomial nature. Without restricting the generality, one might assume that they are the same. Indeed, one might always redefine the systems of basis functions $\{X_m\}$ and $\{Y_m\}$ as $\{\mathrm{X_m}\} \cup \{\mathrm{Y_m}\}$. In this case, the equations can be rewritten as

$$\int\int\int_V \left[C_{ijkl}^q(u_{(k,l)}^r + u_{(k,l)}^s - \Delta T \alpha_{kl}^q)\right] X_{m,j}\,\mathrm{d}V = \int\int_{S_T} T_i X_m\,\mathrm{d}S, \tag{13a}$$

$$\int\int\int_V \left[C^q_{ijkl}u^s_{(k,l)}\right]X_{m,j}\,\mathrm{d}V = \int\int\int_V \sigma^{\mathrm{hyb}}_{ij}X_{m,j}\,\mathrm{d}V. \tag{13b}$$

Integrating by parts and adding the equations to each other, one obtains

$$\int\int\int_V \left[C^q_{ijkl}u^r_{(k,l),j} + \sigma^{\mathrm{hyb}}_{ij,j}\right]X_m\,\mathrm{d}V + \int\int_{S_T}[T_i - (C^q_{ijkl}(u^r_{(k,l)} - \Delta T\,\alpha^q_{ij}) + \sigma^{\mathrm{hyb}}_{ij})n_j]X_m\,\mathrm{d}S = 0.$$

The first term of the above equation contains the weak form of the equilibrium equations and the second term, the weak form of the boundary conditions. They are interconnected, meaning that if the boundary conditions are not satisfied in the weak form, [2] then the error in the equilibrium equations will not vanish even in the weak form, i.e. it will not be orthogonal to each of the displacement approximation basis functions. In Section 5, a form of $\sigma^{\mathrm{hyb}}_{ij}$ will be proposed so that the boundary conditions on the hole edge and the interfacial continuity conditions, will be satisfied. In this case, provided that Eqs. (13a) and (13b) are also satisfied, the stresses (8) will satisfy the equilibrium equations in the weak sense, even in the vicinity of the singularities.

5. Hybrid approximation

Consider the exact stresses associated with the displacement u^s_i in the qth ply:

$$\sigma^s_{ij} = C^q_{ijkl}u^s_{(k,l)}.$$

The thermal expansion term is not included with the singular displacement portion, since it was accounted for in Eq. (9). The stresses resulting from displacement field u^s_i are modified to include the singular asymptotic stress field (6). We shall calculate the strain field generated by the truncated derivatives of the displacements, as follows:

$$2u^s_{(i,j)_\theta} = \left(\frac{\partial u^s_i}{\partial x_j}\right)_\theta + \left(\frac{\partial u^s_j}{\partial x_i}\right)_\theta,$$

where $\left(\partial u^s_i/\partial x_j\right)_\theta$ are calculated according to truncated expressions (4). The contribution of the stresses generated by these strains is given by the asymptotic stress field (6), so that the hybrid stresses associated with displacements u^s_i are

$$\sigma^{\mathrm{hyb}}_{ij} = \sigma^s_{ij} + \sum_{p=1}^{N-1}K_p(\theta)a^p_{ij} - s_{ij},$$

where

$$s_{ij} = C^q_{ijkl}u^s_{(k,l)_\theta}. \tag{14}$$

The unknown functions of the hybrid approximation (7) and (8) are the displacements u^s_i, u^r_i and coefficients K_p. Practically speaking, we expect the hybrid approximation to be needed only in the vicinity of the hole edge. The size of this region is a solution parameter. In the superposition context, it is intuitive that its size needs to be sufficiently large so that the spline approximation would be capable of approximating the asymptotic term accurately on the outer (with respect to the hole edge) boundary of this region. A numerical study will be performed to illustrate the insensitivity of the results to the size of this region. Let the volume Γ be bounded by the hole edge, the top and bottom surfaces and $r = r_0$: $D/2 < r_0 < \min(L, A)$.

[2] The error is orthogonal to each of the displacement approximation basis functions.

Inside this region stresses are given by Eq. (8), and outside this region $u_i^s = 0$ and $\sigma_{ij} = \sigma_{ij}^r$. The total displacement must be continuous at the internal boundary $r = r_0$. It can be satisfied easily if the unknown displacement approximation functions are the total displacement u_i and u_i^s instead of u_i^r and u_i^s. The stress approximation (8) can be rewritten accordingly:

$$\sigma_{ij} = \sigma_{ij}^u + \sum_{p=1}^{N-1} K_p(\theta) a_{ij}^p - s_{ij}, \tag{15}$$

where

$$\sigma_{ij}^u = C_{ijkl}^q (u_{(k,l)} - \alpha_{kl}^q \Delta T). \tag{16}$$

6. Governing equations

Taking into account Eqs. (15) and the change to independent displacement functions u_i and u_i^s, Eqs. (13a) and (13b) will attain the following form:

$$\int\int\int_V \left[C_{ijkl}^q (u_{(k,l)} - \Delta T \alpha_{kl}^q) \right] X_{m,j} \, \mathrm{d}V = \int\int_{S_T} T_i X_m \, \mathrm{d}S, \tag{17}$$

$$\int\int\int_\Gamma \left[C_{ijkl}^q u_{(k,l)_\theta}^s \right] X_{m,j|\theta} \, \mathrm{d}V = \int\int\int_\Gamma \sum_{p=1}^{N-1} K_p(\theta) a_{ij}^p X_{m,j|\theta} \, \mathrm{d}V, \tag{18}$$

where $X_{m,j|\theta}$ are based on truncated derivatives (4). Eq. (17) follows from Eq. (13a) after substituting Eq. (7) and allows one to calculate the total displacement in an independent problem under the given traction and displacement boundary conditions (1). Several steps have been undertaken to reduce Eq. (13b) to Eq. (18). It has been considered that the hybrid approximation is defined inside Γ only and that truncated derivatives (4) were used in the hybrid stress approximation. The spatial derivatives appearing in Eq. (18) are also truncated derivatives, meaning that auxiliary problem (18) is a two-dimensional problem with the θ-coordinate as a parameter. A substitution

$$u_i^s = \sum_{p=1}^{N-1} K_p u_i^{s,p}$$

provides a solution of Eq. (18) for arbitrary K_p if

$$\int\int\int_\Gamma \left[C_{ijkl}^q u_{(k,l)_\theta}^{s,p} \right] X_{m,j|\theta} \, \mathrm{d}V = \int\int\int_\Gamma a_{ij}^p X_{m,j|\theta} \, \mathrm{d}V, \quad p = 1, \ldots, N-1. \tag{19}$$

The displacement boundary conditions on the singular components $u_i^{s,p}$ must exclude rigid body motion and be consistent with Eq. (5), i.e. no surface displacements can be prescribed for $u_i^{s,p}$ on $S_T \cap \partial\Gamma$. Eq. (19) provides the weak form of the equality of tractions $a_{ij}^p n_j$ and $C_{ijkl}^q u_{(k,l)_\theta}^{s,p} n_j$ on the portion of $\partial\Gamma$ inside the laminate ($r = r_0$), provided that no surface displacements are prescribed for $u_i^{s,p}$ there. If the distance between this boundary and the hole edge is chosen sufficiently large then the resulting traction discontinuity at this boundary for the stress field (15) may be reduced arbitrarily by increasing the numerical subdivision for the auxiliary problem. The following boundary conditions, consistent with Eq. (5), were imposed

$$u_r^{s,p}(D/2, z^{(p)}, \theta) = u_\theta^{s,p}(D/2, z^{(p)}, \theta) = 0, \qquad u_z^{s,p}(r_0, z^{(p)}, \theta) = 0. \tag{20}$$

The stress approximation after the substitution can be rewritten as

$$\sigma_{ij} = \sigma^u_{ij} + \sum_{p=1}^{N-1} K_p(\theta)(a^p_{ij} - s^p_{ij}), \tag{21}$$

where

$$s^p_{ij} = C^q_{ijkl} u^{s,p}_{(i,j)_\theta}.$$

7. Determination of $k_p(\theta)$

The error in boundary conditions near the singularity from Eq. (17) is a result of approximating the directionally non-unique singular stress field by polynomials. The directional non-uniqueness means that for $\eta \to 0$, the stresses a^p_{ij} may tend to $\pm\infty$ depending upon ψ. The polynomial approximation provides unique and finite stress values at every point of a given ply. The values of the stress intensity factors are obtained to enforce singlevaluedness of the non-singular portion

$$\sigma^u_{ij} - K_p(\theta) s^p_{ij} + \sum_{\substack{q=1,\\ q\neq p}}^{N-1} K_q(\theta)(a^q_{ij} - s^q_{ij})$$

at the singular point. Consider the interface $z = z^{(p)}$ between the p and the $p+1$st ply. Let $P^{(p)}_i(\eta)$ be the interlaminar traction on the interface $z = z^{(p)}$ in the vicinity of the edge ($P^{(p)}_i(0) = \pm\infty$). Then, at the hole edge, six traction boundary conditions have to be simultaneously satisfied

$$T_i = \sigma_{ij} n^h_j, \qquad P^{(p)}_i(\eta) = \sigma_{ij} n^p_j.$$

Thus, one stress component, namely σ_{rz}, will appear in two equations which are

$$T_z = \sigma_{rz}\left(\eta, \pm\frac{\pi}{2}, \theta\right), \qquad P^{(p)}_r(\eta) = \sigma_{rz}(\eta, 0, \theta).$$

These equations can only be satisfied if

$$\begin{aligned}\lim_{\eta\to 0}\left[T_z - K_p(\theta) a^p_{rz}\left(\eta, \frac{\pi}{2}, \theta\right)\right] &= \lim_{\eta\to 0}[P_r - K_p(\theta) a^p_{rz}(\eta, 0, \theta)] \\ &= \sigma^u_{rz}\left(\frac{D}{2}, z^{(p)}, \theta\right) - K_p(\theta) s^p_{ij}\left(\frac{D}{2}, z^{(p)}, \theta\right) \\ &\quad + \sum_{\substack{q=1,\\ q\neq p}}^{N-1} K_q(\theta)\left[a^q_{ij}\left(\frac{D}{2}, z^{(p)}, \theta\right) - s^q_{ij}\left(\frac{D}{2}, z^{(p)}, \theta\right)\right].\end{aligned} \tag{22}$$

These equations are necessary conditions to make the polynomial part of the stress tensor single valued. It is worth noting that if instead of a corner one has a crack, i.e. $n^h_i = -n^p_i$, then we shall have three pairs of single-valuedness conditions, one per each stress component in the plane normal to the crack. It will require three stress intensity factors: Modes I–III. In the case of a hole edge, we have only one interlaminar stress component which requires the single-valuedness condition – σ_{rz}. The criterion for determining $K_p(\theta)$ will be the continuity of the non-singular part of σ_{rz} stress component at the singular points, i.e.

$$\Delta\left[\sigma_{ij}^{u}\left(\frac{D}{2},z^{(p)},\theta\right)\right]=K_p(\theta)\,\Delta\left[s_{ij}^{p}\left(\frac{D}{2},z^{(p)},\theta\right)\right]+\sum_{\substack{q=1,\\ q\neq p}}^{N-1}K_q(\theta)\,\Delta\left[a_{ij}^{q}\left(\frac{D}{2},z^{(p)},\theta\right)-s_{ij}^{q}\left(\frac{D}{2},z^{(p)},\theta\right)\right],\quad p=1,\ldots,N-1, \tag{23}$$

where $\Delta[\ ]$ denotes the difference of the bracketed function between $z^{(p)}+0$ and $z^{(p)}-0$. The non-diagonal terms in the right-hand side of Eq. (23) represent the influence of the singularities of adjacent plies. These terms will become small if the subdivision of the p and $p+1$ is dense as the non-diagonal terms contain the difference between the asymptotic solution and its polynomial approximation away from the singularity. However, for coarse subdivisions, the contribution of the adjacent plies is significant for convergence.

8. Spline approximation of displacement components

The x, y and z displacement components are approximated by using cubic spline functions in curvilinear coordinates. The total displacement is approximated as

$$u_i=\mathbf{C}_i\mathbf{X}\mathbf{U}_i^{\mathrm{T}}+\delta_{i1}u_0\mathbf{X}\mathbf{E}^{\mathrm{T}}, \tag{24}$$

where $\mathbf{X}$ is a vector of three-dimensional spline approximation basis functions, and $\mathbf{U}_i$ are the unknown spline approximation coefficients. The non-square matrices $\mathbf{C}_i$ and constant vector $\mathbf{E}$ are defined so that approximation (24) is kinematically admissible, i.e., it satisfies boundary conditions (1) for arbitrary coefficients $\mathbf{U}_i$. Bold type will be used to distinguish vectors and matrices; superscript T means the transpose operation.

A detailed description of the spline approximation procedure and the properties of spline functions are given by Iarve (1996). The three-dimensional spline approximation functions are defined in curvilinear coordinates. The x,y plane was mapped into a region defined by ρ, ϕ, where $0\leqslant\rho\leqslant1$ and $0\leqslant\phi\leqslant2\pi$. The transformation was defined as follows:

$$\begin{aligned}x&=\frac{D}{2}F_1(\rho)\cos\phi+LF_2(\rho)\alpha(\phi)+x_{\mathrm{c}},\\ y&=\frac{D}{2}F_1(\rho)\sin\phi+AF_2(\rho)\beta(\phi)+y_{\mathrm{c}}.\end{aligned} \tag{25}$$

Functions F_1 and F_2 were defined as

$$F_1(\rho)=\begin{cases}1+\kappa\rho, & \rho\leqslant\rho_{\mathrm{h}},\\ \frac{(1+\kappa\rho_{\mathrm{h}})(1-\rho)}{1-\rho_{\mathrm{h}}}, & \rho_{\mathrm{h}}\leqslant\rho\leqslant1,\end{cases}\qquad F_2(\rho)=\begin{cases}0, & \rho\leqslant\rho_{\mathrm{h}},\\ \frac{\rho-\rho_{\mathrm{h}}}{1-\rho_{\mathrm{h}}}, & \rho_{\mathrm{h}}\leqslant\rho\leqslant1.\end{cases}$$

Coordinate line $\rho=0$ describes the contour of the hole, and the coordinate line $\rho=1$ describes the rectangular contour of the plate. Parameter κ defines the size of a near-hole region $D/2\leqslant r\leqslant(1+\kappa)D/2$, which corresponds to $0\leqslant\rho\leqslant\rho_{\mathrm{h}}$, where a simple relationship between the polar coordinates and the curvilinear coordinates ρ, ϕ exists

$$r-\frac{D}{2}=\frac{D\kappa}{2}\rho\quad\text{and}\quad\theta=\phi. \tag{26}$$

The width of this region is typically one hole radius, i.e., $\kappa\rho_{\mathrm{h}}=1$. Beyond this region a transition between the circular contour of the opening and the rectangular contour of the plate is performed. Functions $\alpha(\phi)$

and $\beta(\phi)$ describing the rectangular contour of the plate boundary were given by Iarve (1996). These functions are introduced so that parametric equations $x = \alpha(\phi) + x_c,\ y = \beta(\phi) + y_c$ describe the rectangular contour of the plate, and $0 \leqslant \phi < \phi^{(1)}$ corresponds to $0 < x \leqslant L,\ y = A;\ \phi^{(1)} \leqslant \phi < \phi^{(2)}$ corresponds to $x = 0,\ 0 < y \leqslant A;\ \phi^{(2)} \leqslant \phi < \phi^{(3)}$ corresponds to $0 \leqslant x < L,\ y = 0$; and $\phi^{(3)} \leqslant \phi < 2\pi$ corresponds to $x = L,\ 0 \leqslant y < A$.

Sets of one-dimensional cubic spline functions were defined in each coordinate direction. Subdivisions were introduced through the thickness of each ply such that the pth ply, which occupies a region $z^{(p)} \leqslant z \leqslant z^{(p-1)}$, is subdivided into n_p sublayers. A set of $N_z = \sum_{p=1}^{N} n_p + 2N + 1$ basic B-type cubic spline functions $\{Z_i(z)\}_{i=1}^{N_z}$ with variable defect was built along the z-coordinate according to a recurrent procedure given by Iarve (1996). These cubic splines are twice continuously differentiable at all nodal points inside each ply and have discontinuous first derivatives (the function itself is continuous) at the ply interfaces to account for interfacial strain discontinuities. This is a necessary condition for traction continuity at the ply interfaces. Nodal points are also introduced in the ρ and ϕ directions as follows: $0 = \rho_0 < \rho_1 < \cdots < \rho_m = 1,\ 0 = \phi_0 < \phi_1 < \cdots < \phi_k = 2\pi$. The subdivision of the ρ coordinate is non-uniform. The interval size increases in geometric progression beginning at the hole edge. The region $0 \leqslant \rho \leqslant \rho_h$ wherein the curvilinear transformation is cylindrical is subdivided into m_1 intervals ($m_1 < m$), so that $\rho_h = \rho_{m_1}$. Sets of basic cubic spline functions $\{R_i(\rho)\}_{i=1}^{m+3},\ \{\Phi_i(\phi)\}_{i=1}^{k+3}$ along each coordinate are built so that twice continuous derivatives in each node are provided. Splines along the ϕ are periodic at the ends of the interval. The vector of the three-dimensional spline approximation functions was defined as the tensor product of three one-dimensional sets of splines:

$$\{X\}_q = R_i(\rho)\Phi_j(\phi)Z_l(z), \quad q = l + (j-1)N_z + (i-1)N_z k, \quad l = 1, \ldots, N_z,\ j = 1, \ldots, k,$$
$$i = 1, \ldots, m+3.$$

The components of vector $\mathbf{E}$ are equal to 1 or -1 for a component of $\mathbf{X}$ that is non-zero at $\rho = 1,\ \phi^{(1)} \leqslant \phi < \phi^{(2)} (x = 0)$ and $\rho = 1,\ \phi^{(3)} \leqslant \phi < 2\pi\ (x = L)$, respectively. All other components of the vector $\mathbf{E}$ are equal to zero. The boundary matrices are obtained by deleting a number of rows from the unit matrix. The deleted rows have non-zero scalar product with $\mathbf{E}$.

The region Γ of the hybrid approximation superposition is inside the region in which transformation (25) coincides with Eq. (26). The boundary $r = r_0$ is defined to coincide with the radial coordinate line so that $r_0 = (D/2)(1 + \kappa\rho_{m_0})$, where $m_0 \leqslant m_1$. A reduced set of splines in the ρ-direction $\{R_i^s(\rho)\}_{i=1}^{m_h+3}$ is defined only over the first m_1 intervals for the purposes of efficient solution of the systems of equations for determining $u_i^{s,p}$. It is built exactly the same way as the one over the entire interval. It can be shown that the reduced set is a subset of approximation (24).

The approximation of the singular displacements can be written as

$$u_i^{s,p} = \mathbf{C}_i^p \mathbf{X}^s \mathbf{U}_i^{p^T}, \tag{27}$$

where $\mathbf{U}_i^p(\theta)$ are unknown coefficients and

$$\{\mathbf{X}^s\}_q = R_i^s(\rho)Z_l(z), \quad q = l + (i-1)N_z, \quad l = 1, \ldots, N_z,\ j = 1, \ldots, k,\ i = 1, \ldots, m_1 + 3.$$

Matrices $\mathbf{C}_i^p$ are defined to satisfy boundary conditions (20). The truncated in-plane derivatives in Eq. (19) are calculated as

$$\left(\frac{\partial}{\partial x}\right)_\theta = \frac{2}{D\kappa}\cos\phi\frac{\partial}{\partial\rho}, \qquad \left(\frac{\partial}{\partial y}\right)_\theta = \frac{2}{D\kappa}\sin\phi\frac{\partial}{\partial\rho},$$

9. Numerical results

9.1. [45/−45]$_s$ laminate

A square [45/−45]$_s$ plate similar to that in Wang and Lu (1993) is considered. The geometric properties are $L = A = 0.508$ M, $x_c = y_c = L/2, D = 0.0508$ M, and ply thickness $h = 0.00254$ M. Orthotropic ply properties were $E_1 = 138$ GPa, $E_2 = E_3 = 14.5$ GPa, $G_{12} = G_{13} = G_{23} = 5.86$ GPa, and $\nu_{12} = \nu_{13} = \nu_{23} = 0.21$, where index 1 corresponds to the fiber direction, and ν_{ij} the poisson ratio meaning strain ε_i under uniaxial stress σ_j in contracted notations. The displacement boundary conditions (1) were applied so that $u_0/L = 0.001$. The average applied stress was calculated as

$$\sigma_0 = \frac{1}{AH}\int_0^A \int_0^H \sigma_{xx}(L, y, z)\,\mathrm{d}y\,\mathrm{d}z.$$

Several modes of subdivision were used for the convergence study. The θ coordinate in all cases was uniformly divided into 48 intervals. The coarse mesh was chosen so that

z-coordinate: $n_s = 1$ – one sublayer per ply.

ρ-coordinate: a total of $m = 12$ intervals, with $m_1 = 8$ intervals in the cylindrical transformation region, which was a hole radii wide ($\kappa\rho_h = 1$). The consecutive interval length ratio was $q = 1.2$, where $q = (\rho_{i+1} - \rho_i)/(\rho_i - \rho_{i-1})$.

The fine subdivision was as follows:

z-coordinate: $n_s = 4$, non-uniform sublayers per ply, sublayer thickness ratio 1.3 with thin sublayers at the interface.

ρ-coordinate: $m = 24$, $m_0 = 20$, $\kappa\rho_h = 1$, $q = 1.4$.

First, the influence of the width of the region Γ on $k(\theta)$ is investigated. The coarse mesh was considered. The width of the region m_h was changed from 1 to 8 int. The $K(\theta)/\sigma_0$, in units $(0.0254\ \mathrm{M})^{(1-\lambda(\theta))}$, obtained by using Eq. (23) is shown in Fig. 2a for $m_0 = 1,2,8$. Starting with $m_0 = 2$ the $K(\theta)$ values are practically unchanged. It should be noted that the minimum value even for $m_0 = 1$ differs from the value obtained for $m_0 \geqslant 2$ by less than 5%. In all of the following results $m_0 = 6$. Fig. 2b illustrates the influence of the density of subdivision on the $K(\theta)$ values. The results obtained with coarse and fine subdivisions are very close. A fairly close, but not precise, agreement between the present results and Wang and Lu (1993) also shown in Fig. 2b, is observed.

Stress values obtained by using the hybrid approximation will be illustrated below. The stresses σ_{rz} and σ_{zz} in the cross-section $\theta = 90°$ will be considered at the interfacial surface. The shear stress σ^u_{rz} distribution calculated from the total displacements by using Eq. (17), is shown in Fig. 3a for two different subdivisions. For distances from the hole edge smaller than $0.2H$ and $0.8H$ for the finer and coarser subdivisions, respectively, the shear stress is discontinuous at the interface. Mesh refinement will further shrink the distance at which the discontinuity is evident; however, the stress values at the hole edge on the two-ply surfaces will diverge even more. This behavior is readily understood by examining the asymptotic stress functions in Fig. 4, after which we will return to discuss Fig. 3b.

Functions $a_{ij}(1, \psi, 90°)$ are shown in Fig. 4, where the coordinates are (η, ψ, θ). Two ordinate scales are utilized due to a difference in magnitudes of the a_{zz}, and $a_{z\theta}$ functions and all other functions. The angular distribution of the shear component $a_{rz}(1, \psi, 90°)$ satisfies the zero traction boundary conditions at the hole surfaces $\psi = \pm\pi/2$ and the continuity condition at the interface $\psi = 0$. In addition, the stress amplitude along the interface is zero, not infinite, if the singular point is approached in this direction. At $-\pi/2 < \psi < 0$ and $0 < \psi < \pi/2$, however, the same stress component is unbounded at the singular point and tends towards $-\infty$ in the lower ply and $+\infty$ in the upper ply. The directional non-uniqueness of the solution is reflected by diverging interlaminar shear stress values observed by using the polynomial approximation (Fig. 3a). The stresses calculated by using hybrid approximation (21) in conjunction with

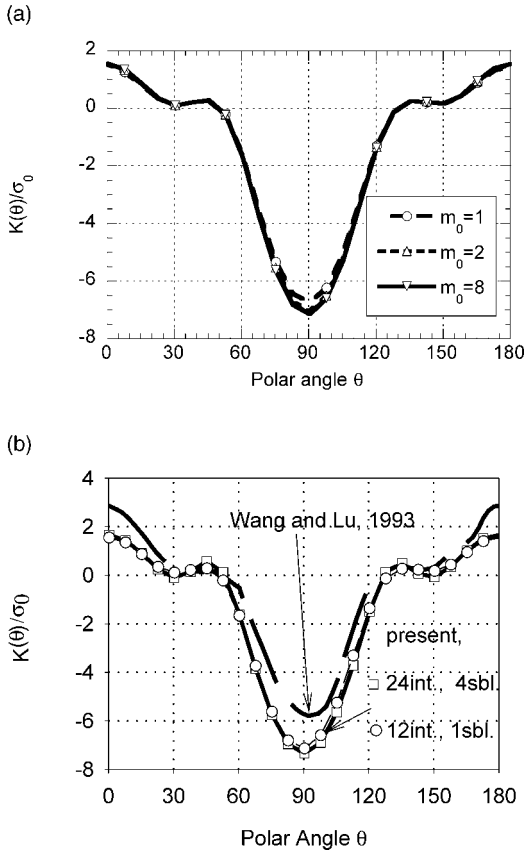

Fig. 2. (a) Values of $K(\theta)$ at the ± 45 interface versus size of the hybrid approximation region. (b) Values of $K(\theta)$ for different subdivision densities and comparison with Wang and Lu (1993).

Eq. (18), are shown in Fig. 3b and clearly indicate convergence with mesh refinement. Note that the stress displayed in this figure is at the same time the pure polynomial part of the hybrid stress, since $a_{rz}(\eta, 0, 90^\circ) = 0$. Thus, by approaching the singular point along the hole edge, we will again recover the zero value.

The transverse normal stress component will be considered next. As seen in Fig. 4, it exhibits a practically constant directional amplitude in the $\theta = 90^\circ$ cross-section. The stress values σ_{zz} defined through the total displacement field by using the same two meshes as before are shown in Fig. 5a. For both meshes, no discontinuity between the stress values in the two plies at the interface can be seen. Thus, the natural boundary condition – interfacial continuity of the transverse normal stress component, is satisfied quite accurately. However, the stress values obtained using the coarse and the fine mesh are different in the hole edge vicinity. Fig. 5b displays the function

$$K(\theta)(a_{zz}^1 - s_{zz}^1)/\sigma_0,$$

which is superimposed with the displacement-based stress value σ_{zz}^u in Eq. (21). For the fine mesh, it has a non-zero value only in the very vicinity of the singularity and extends to up to $0.8H$ away from the hole

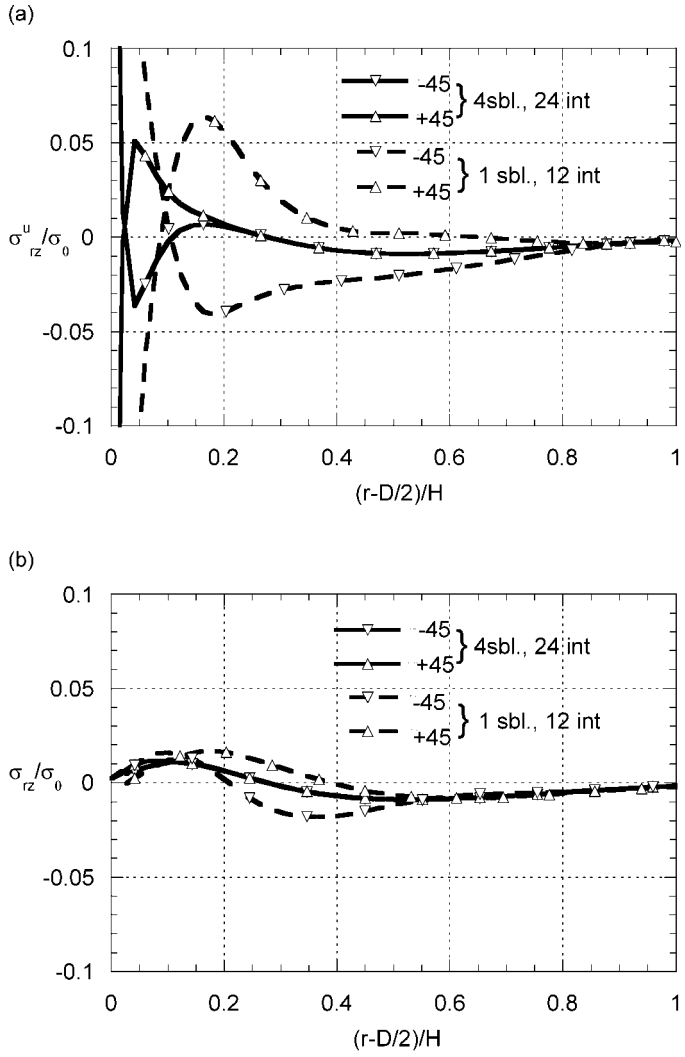

Fig. 3. Transverse interlaminar shear stress at $\theta = 90°$.

edge for the coarse mesh. The hybrid stress values σ_{zz} for the two meshes are shown in Fig. 5c and display a good agreement.

The transverse shear stresses $\sigma^u_{z\theta}$ and $\sigma_{z\theta}$ are shown in Fig. 6a and b, respectively. For this stress component, the $\sigma^u_{z\theta}$ results obtained with the two meshes show the smallest difference. However, the hybrid approximation clearly provides a more convergent solution for this stress component also.

9.2. Uniaxial tension of $[45/90/-45/0]_s$ laminate

A $[45/90/-45/0]_s$ quasi-isotropic IM7/5250-2 laminate was considered next, where the stacking order is from the top to the central plane, reading from left to right, respectively. The elastic properties of the unidirectional ply were $E_1 = 151$ GPa, $E_2 = E_3 = 9.45$ GPa, $G_{12} = G_{13} = 5.9$ GPa, $G_{23} = 3.26$ GPa,

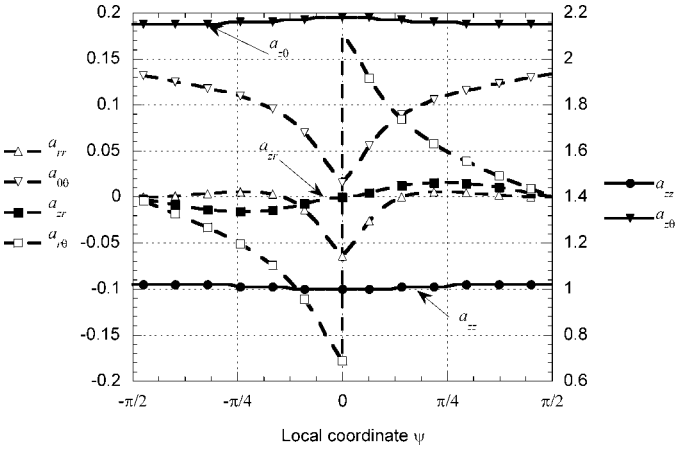

Fig. 4. Amplitudes of asymptotic stress functions at $\theta = 90°$.

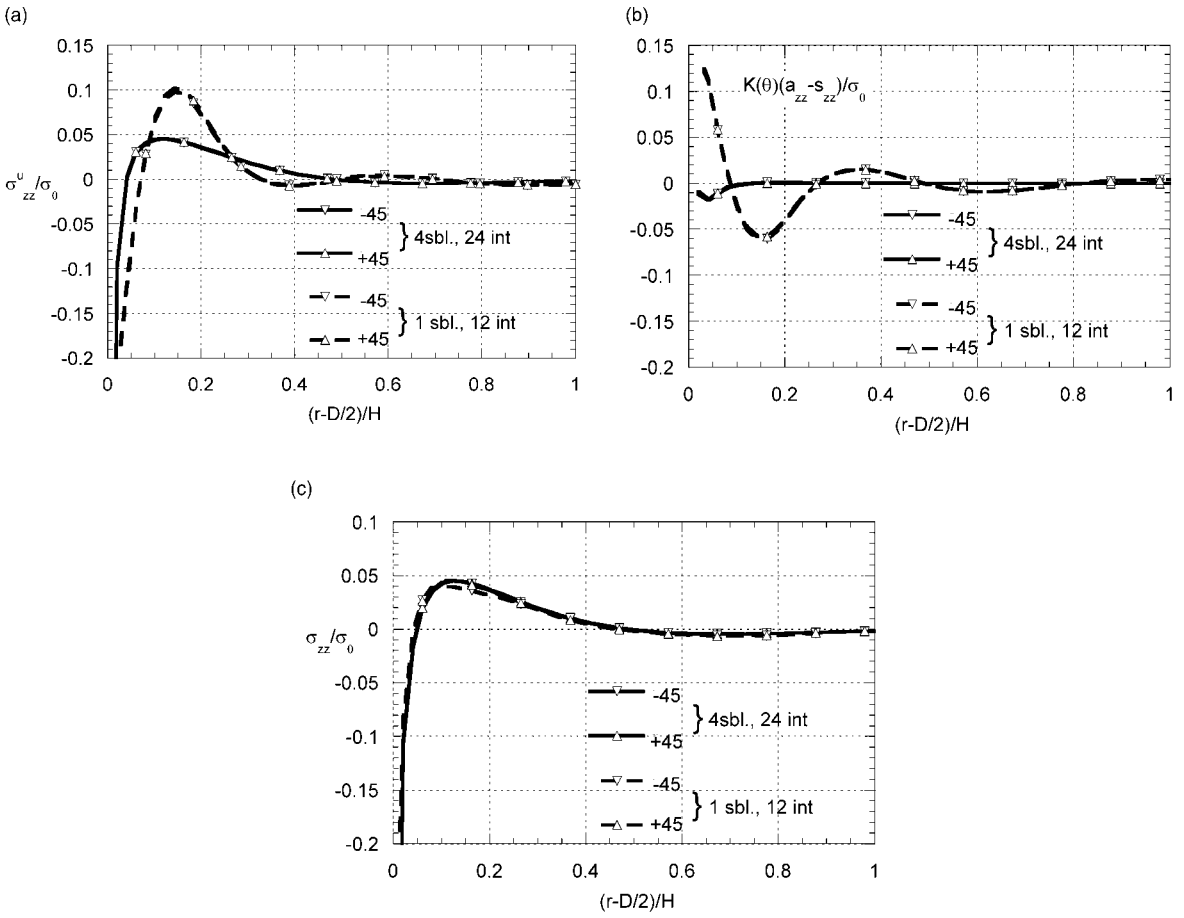

Fig. 5. Transverse interlaminar normal stress at $\theta = 90°$.

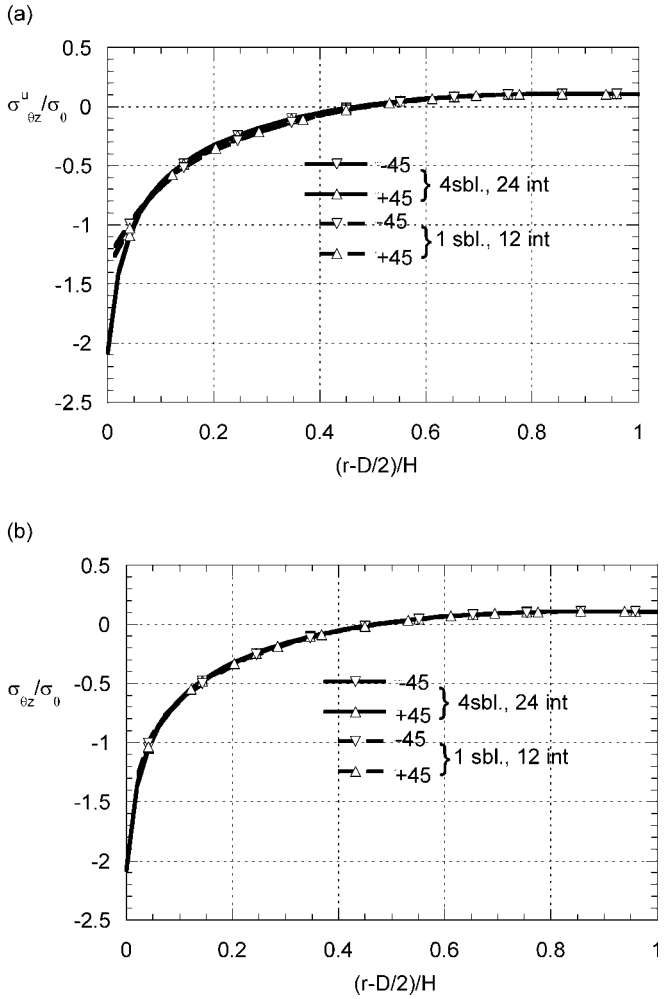

Fig. 6. Transverse interlaminar shear stress at $\theta = 90°$.

$v_{12} = v_{13} = 0.32$, and $v_{23} = 0.45$. The in-plane dimensions of the plate were $L = 0.29$ M, $A = 0.076$ M, $x_c = L/2$, $y_c = A/2$, $D = 0.0125$ and the ply thickness $h = 0.00134$ M. Fig. 7 shows the power of singularity calculated for each interface as a function of the polar angle; it varies for stresses from –0.01 to –0.077 depending on the angle. Two mesh densities were used for obtaining the coefficient of the singular term under the uniaxial loading boundary conditions. Coarse subdivision was defined as follows:

z-coordinate-1 sublayer per ply,

ρ-coordinate-m = 12, $m_0 = 8$, $\kappa\rho_h = 1$, $q = 1.2$,

θ-coordinate-48 equal intervals.

The fine subdivision consisted of

z-coordinate-three non-uniform (1:2:1) sublayers per ply,

ρ-coordinate-m = 24, $m_0 = 20$, $\kappa\rho_h = 1$, $q = 1.2$,

θ-coordinate-48 equal intervals.

The coefficient of the singular stress term calculated by using these subdivisions is shown in Fig. 8 at each interface. The values obtained by using Eq. (23) and the values calculated by retaining only the diagonal

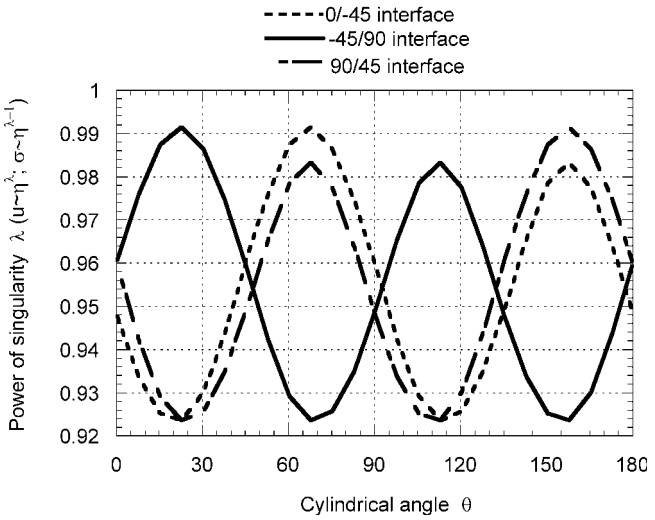

Fig. 7. Power of singularity versus cylindrical angle at all interfaces of the $[45/90/-45/0]_s$ laminate.

terms on the right-hand side of Eq. (23) are compared. For the coarse subdivision, the non-diagonal terms are very significant, so that the values obtained by neglecting them may even be of a different sign. For the fine subdivision, the two results are almost identical. Indeed, the magnitudes of the non-diagonal terms are determined by the accuracy of approximation of the singular stress term by the polynomial approximation one or more ply thicknesses away from the singularity. The density of the subdivision through the ply thickness defines this accuracy. The values of the K_4, K_5 and K_6 obtained with the two subdivisions and taking into account the non-diagonal terms are close together. Fig. 9 shows the characteristics of the singular behavior of the interlaminar shear stresses, namely:

$$\lim_{\eta\to 0}\eta^{1-\lambda}\sigma_{z\theta}(D/2+\eta,z^{(p)},\theta)=K_p a^p_{z\theta}(1,0,\theta),$$
$$\lim_{\eta\to 0}\eta^{1-\lambda}\sigma_{zr}(D/2+\eta,z^{(p)},\theta)=K_p a^p_{zr}(1,0,\theta),$$

where K_p were determined by the fine mesh solution.

Interlaminar stress components at a $\theta=60.3°$ cross-section will be considered in Figs. 10–13. The transverse radial shear component on all interfaces calculated by using the fine subdivision is shown in Fig. 10. Stresses σ^u_{rz} are displayed in Fig. 10a. At the 0/−45 and −45/90 interfaces, we observe the typical discontinuity of σ^u_{rz}, near the singularity, whereas the interface 90/45 shows a relatively continuous traction up to the singular point. This is in agreement with Fig. 9c showing very small amplitude of the singular term at the latter interface compared to the two others at $\theta=60.3°$. The stresses calculated according to hybrid approximation (21) are shown in Fig. 10b. It should be noted that the point closest to the singularity shown in this figure is $r=D/2+0.002H$. The traction discontinuity is practically indistinguishable within the graphic resolution.

The transverse normal stresses are examined in Figs. 11 and 12. The σ^u_z stresses on all three interfaces are shown in Fig. 11a and b. The difference between the results obtained with two subdivisions are clearly observed for $(r-D/2)/H<0.6$. The values obtained by using the hybrid approximation are displayed in Fig. 12. In this case, the two subdivisions give practically identical results. We observe (Fig. 8c) a small absolute value of K (60.3°) at the 90/45 interface. This led to an inconclusive σ_{zz} trend definition based on Eq. (17) as shown in Fig. 11a. The hybrid approximation in Fig. 12a shows that this interface is in

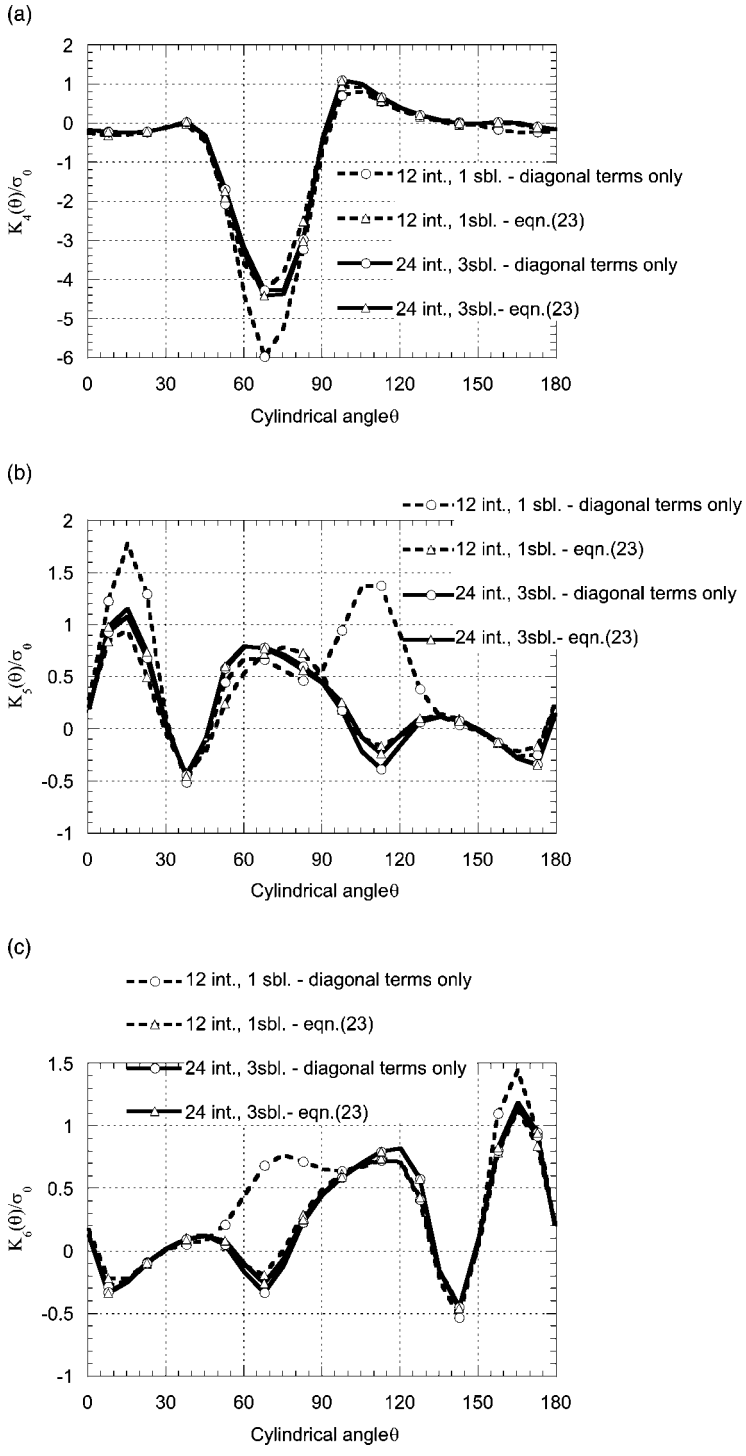

Fig. 8. Singular term coefficients at different interfaces for the $[45/90/-45/0]_s$ laminate under uniaxial loading.

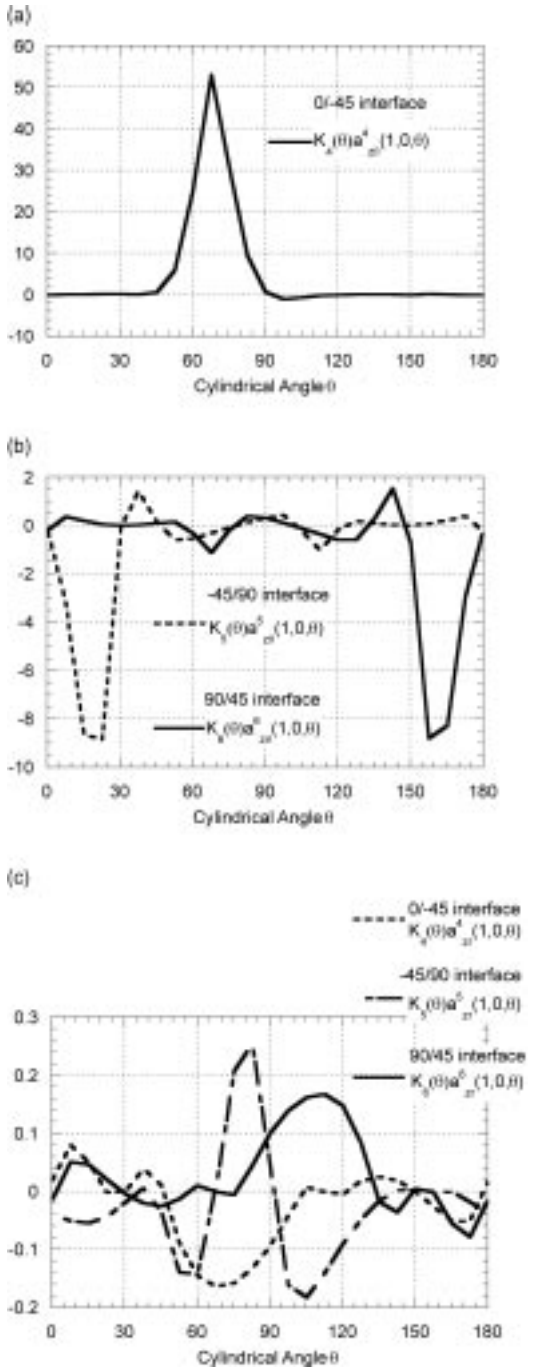

Fig. 9. Transverse shear stress normalized singular term coefficients at different interfaces for the $[45/90/-45/0]_s$ laminate under uniaxial loading.

compression along with the 0/−45 interface. The −45/90 interface exhibits a tensile peel stress singularity, which is in agreement with Fig. 8.

The $\sigma_{z\theta}$ obtained by using the hybrid approximation with the two subdivisions are shown in Fig. 13 for completeness. The fine and the coarse subdivision provide a very close agreement in the stress values which is indicative of convergence.

9.3. Thermal stresses in a $[45/90/-45/0]_s$ laminate

The same laminate is considered under a uniform temperature change of $\Delta T = -167°C$. This temperature drop is used to approximate the residual stresses generated during the processing cool-down phase. The displacement boundary conditions (1) are modified so that the edge $x = L$ is released (zero tractions). The coefficients K_4, K_5 and K_6 obtained with the coarse and fine subdivisions described in the previous section are shown in Fig. 14. Some differences between the coarse and fine mesh analysis results can be seen for low

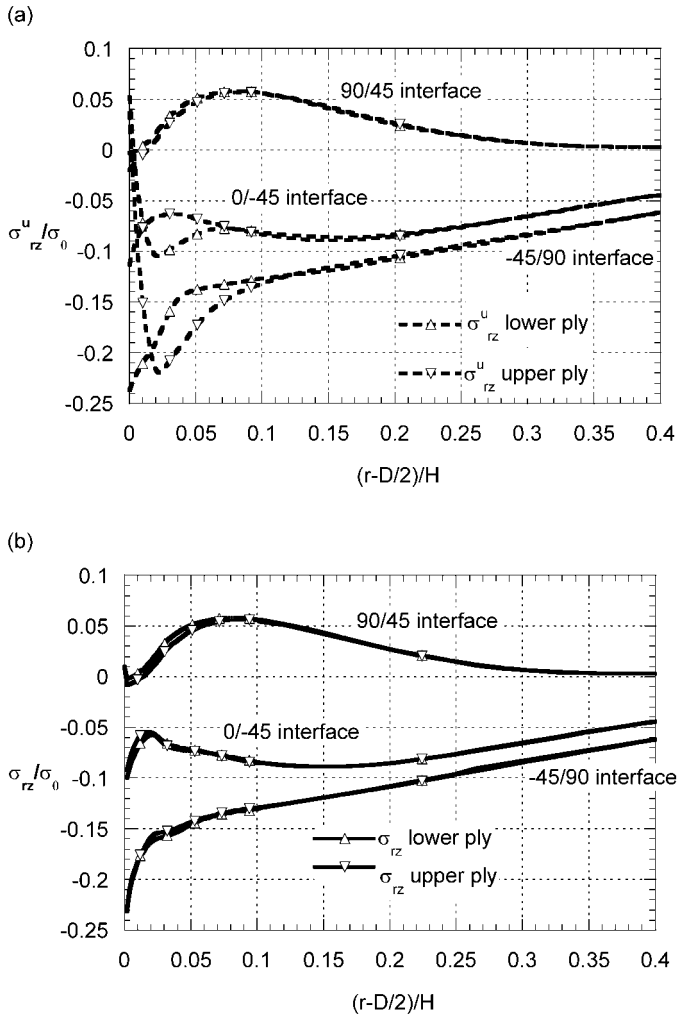

Fig. 10. Transverse interlaminar shear stress at $\theta = 60.3°$.

values, while all the maximum values are practically identical. The values of the coefficients are positive at all interfaces in all circumferential directions. Therefore, a tensile peel stress is expected near singularities. Fig. 15a shows the transverse normal stresses σ^u_{zz} obtained with the coarse subdivision based on displacement approximation in the cross-section $\theta = 157.8°$, where the maximum value of K occurs. The stresses are displayed at two interfaces in the top (solid line) and bottom (dashed line) plies. The normal stresses are seemingly discontinuous a distance of approximately $0.6H$ from the hole edge. Fig. 15b shows the same stresses at all interfaces calculated using the hybrid approximation (21). The discontinuities are reduced significantly. It is interesting to point out that the σ^u_{zz} stress at the 90/45 interface obtained with coarse subdivision in Fig. 15a may appear to have a tendency towards $-\infty$ as one approaches the interface. The hybrid approximation shows a sharp change in sign very close to the singularity. This trend is picked up by the approximation using fine subdivision as shown in Fig. 16a. In this case the tractions at the bottom and top surfaces are continuous starting from $0.2H$ from the hole edge. The hybrid approximation (Fig. 16b) provides traction values with imperceptible discontinuities everywhere. The hybrid stresses obtained with the two subdivisions, Figs. 15b and 16b, are practically the same.

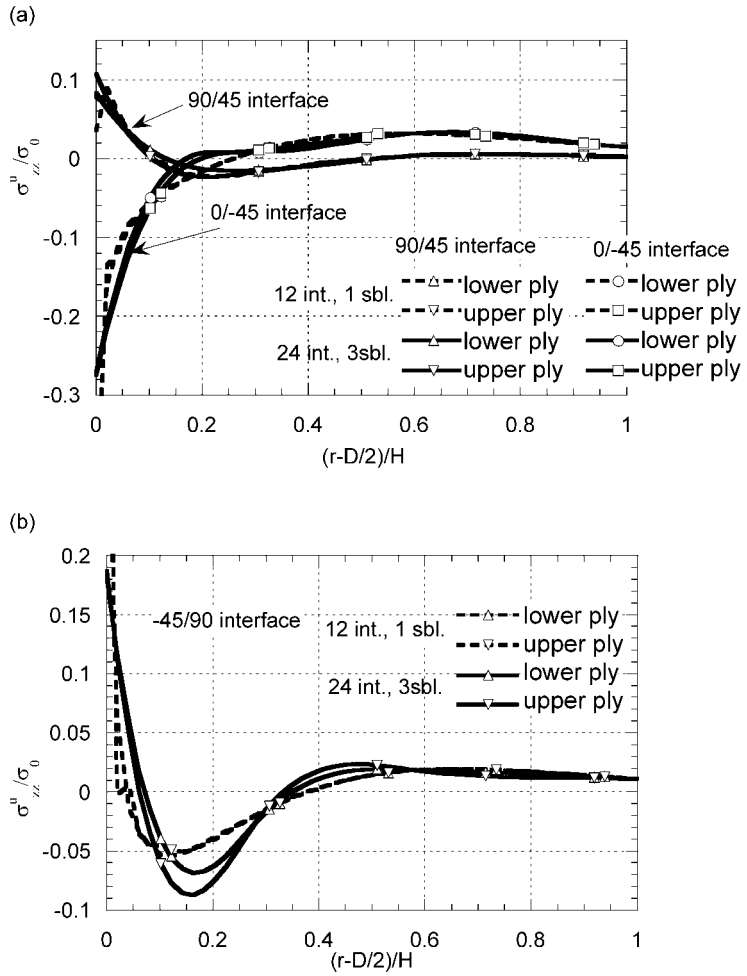

Fig. 11. Transverse interlaminar normal stress at $\theta = 60.3°$ obtained by using displacement approximation.

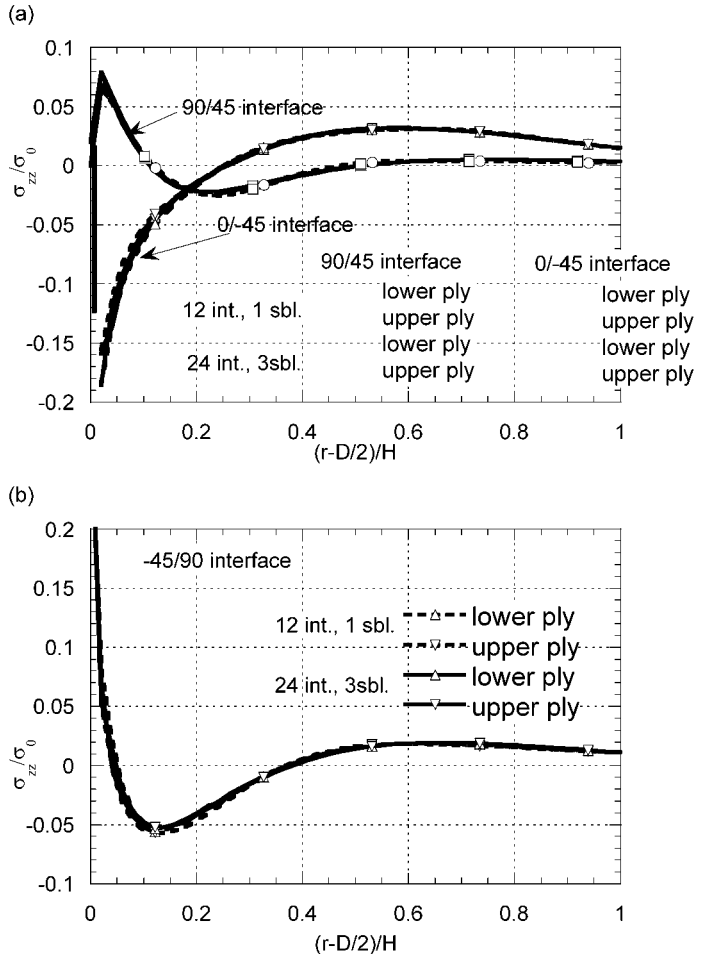

Fig. 12. Transverse interlaminar normal stress at $\theta = 60.3°$ obtained by using hybrid approximation.

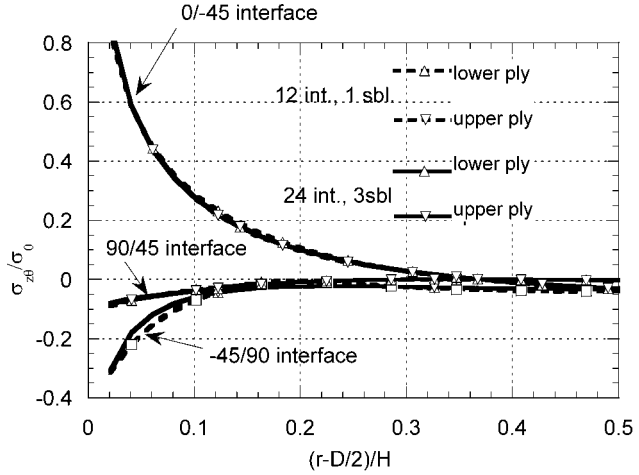

Fig. 13. Transverse interlaminar shear stress at $\theta = 60.3°$.

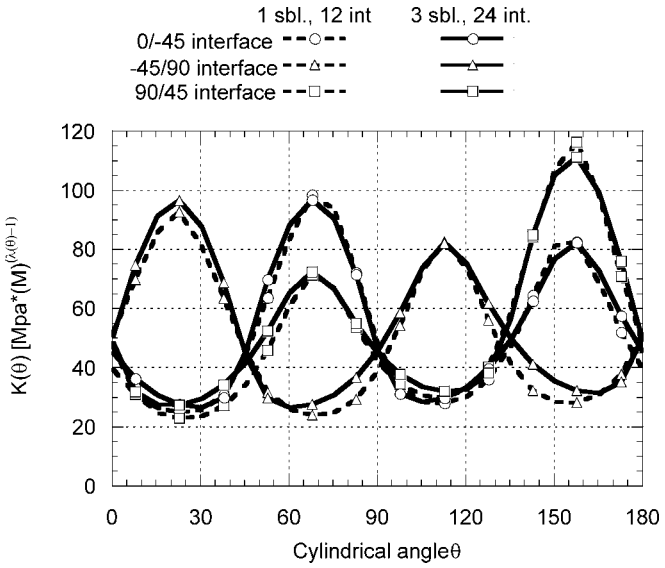

Fig. 14. Singular term coefficients at different interfaces for the $[45/90/-45/0]_s$ laminate under thermal loading.

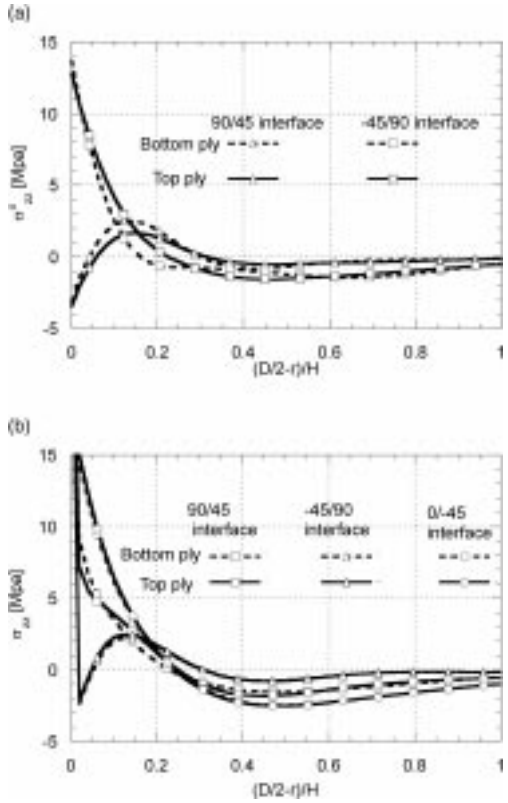

Fig. 15. Transverse interlaminar normal stress at $\theta = 157.3°$ obtained by using displacement approximation with coarse subdivision.

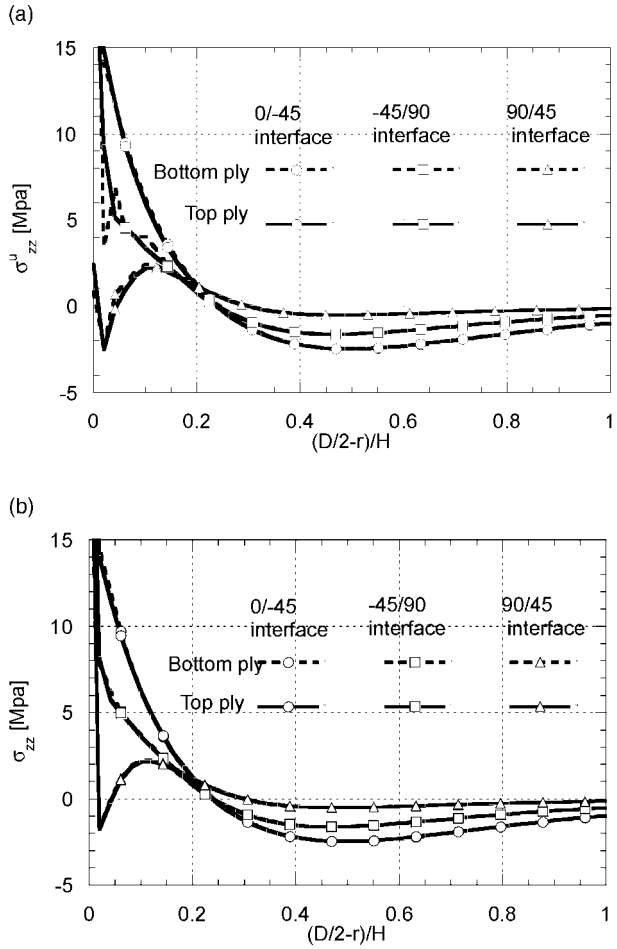

Fig. 16. Transverse interlaminar normal stress at $\theta = 157.3°$ with a fine subdivision.

10. Conclusions

(1) A method of superposition of hybrid and displacement approximations was developed to provide accurate stress fields in the vicinity of the ply interface and the hole edge in a multilayered composite. The asymptotic analysis was used to derive the hybrid stress functions. The displacement approximation was based on polynomial B-spline functions.

(2) The coefficients of the singular terms in stress solution near the ply interfaces and the open-hole edge were determined in $[45/-45]_s$ and quasi-isotropic $[45/90/-45/0]_s$ laminates under mechanical and thermal loading. Convergence studies showed that accurate values of the coefficients of the singular terms can be obtained with the coarse out-of-plane subdivision of one sublayer per ply. It was shown that for laminates with multiple interfaces, the influence of singular terms on adjacent interfaces is important for coarse subdivision convergence.

(3) Converged transverse interlaminar stress components, including their singularities, were shown for $[45/-45]_s$ and $[45/-45/0/90]_s$ laminates under mechanical and thermal loading.

We should make a note of caution that even though accurate representations of singular stresses have been obtained, their physical meaning is open to question since the assumption of homogenization (con-

stant layer thermoelastic moduli) may be invalid in the vicinity of the free edge and ply interface, as shown by Pagano and Rubicki (1974) and discussed by Buryatchenko and Rammerstorfer (1998).

Acknowledgements

The first author acknowledges the support of the Materials Directorate, Air Force Research Laboratory, Wright-Patterson AFB OH under Contract No. F33615-95-D-5029.

Appendix A

$$A_{11} = Q_{11}^{(s)}\cos^2\theta + Q_{16}^{(s)}\sin 2\theta + Q_{66}^{(s)}\sin^2\theta, \qquad A_{12} = Q_{16}^{(s)}\cos^2\theta + \left(Q_{12}^{(s)} + Q_{66}^{(s)}\right)\sin\theta\cos\theta + Q_{62}^{(s)}\sin^2\theta,$$

$$A_{22} = Q_{66}^{(s)}\cos^2\theta + Q_{26}^{(s)}\sin 2\theta + Q_{22}^{(s)}\sin^2\theta, \qquad A_{33} = Q_{55}^{(s)}\cos^2\theta + Q_{54}^{(s)}\sin 2\theta + Q_{44}^{(s)}\sin^2\theta,$$
$$A_{21} = A_{12}, \qquad A_{31} = A_{13} = A_{32} = A_{23} = 0,$$

$$B_{31} = \left(Q_{13}^{(s)} + Q_{55}^{(s)}\right)\cos\theta + \left(Q_{63}^{(s)} + Q_{54}^{(s)}\right)\sin\theta, \qquad B_{32} = \left(Q_{63}^{(s)} + Q_{45}^{(s)}\right)\cos\theta + \left(Q_{23}^{(s)} + Q_{44}^{(s)}\right)\sin\theta,$$
$$B_{21} = B_{12} = B_{11} = B_{22} = B_{33} = 0, \qquad B_{13} = B_{31}, \qquad B_{23} = B_{32},$$

$$C_{11} = Q_{55}^{(s)}, \quad C_{12} = Q_{54}^{(s)}, \quad C_{22} = Q_{44}^{(s)}, \quad C_{33} = Q_{33}^{(s)},$$
$$C_{21} = C_{12}, \quad C_{31} = C_{11} = C_{32} = C_{23} = 0.$$

Ply stiffness coefficients $Q_{ij}^{(s)}$ $s = 1, \ldots, N$ are contracted notations of the fourth order tensor $C_{ijkl}^{(s)}$, used in the text.

References

Buryatchenko, V.A., Rammerstorfer, F.G., 1998. Micromechanics and non-local effects in graded random structure matrix composites. In: Bahei-El Din, Y.A., Dvorak, G.J. (Eds.), IUTAM Symposium on Transformation Problems in Composite and Active Materials. Kluwer Academic Publishers, Dordrecht.

Folias, E.S., 1992. On the interlaminar stresses of a composite plate around the neighborhood of a hole. Int. J. Solids Struct. 25, 1193–1200.

Iarve, E.V., 1996. Spline variational three-dimensional stress analysis of laminated composite plates with open holes. Int. J. Solids Struct. 44 (14), 2095–2118.

Mikhailov, S.E., 1979. Stress singularity in the neighborhood of a rib in a compound inhomogeneous anisotropic body, and some applications to composites. Izv. AN SSR. Mekhanika Tverdogo Tela 49, 103–110.

Morley, L.S.D., 1969. A modification of the Rayleigh–Ritz method for stress concentration problems in elastostatics. J. Mech. Phys. Solids 17, 73–82.

Morley, L.S.D., 1970. A finite element application of the modified Rayleigh–Ritz method. Int. J. Numerical Methods Engng. 2, 85–98.

Pagano, N.J., 1978a. Stress fields in composite laminates. Int. J. Solids Struct. 14, 385–400.

Pagano, N.J., 1978b. Free-edge stress fields in composite laminates. Int. J. Solids Struct. 14, 401–406.

Pagano, N.J., Kaw, A.K., 1995. Asymptotic stresses around a crack tip at the interface between planar or cylindrical bodies. Int. J. Fracture 71, 151–164.

Pagano, N.J., Rubicki, E.F., 1974. On the significance of effective modulus solutions for fibrous composites. J. Composite Mater. 8, 214–228.

Tong, P., Pian, T.H.H., Larsy, S.J., 1973. Hybrid-element approach to crack problems in plane elasticity. Int. J. Numerical Methods Engng. 7, 297–308.

Wang, S.S., Choi, I., 1982. Boundary-layer effects in composite laminates: Parts 1and 2. J. Appl. Mech. 49, 541–560.

Wang, S.S., Lu, X., 1993. Three-dimensional asymptotic solutions for interlaminar stresses around cutouts in fiber composite laminates. In: Rajapakse, Y.D.S. (Ed.), Mechanics of Thick Composites. AMD-vol. 16. Book no. G00785. pp. 41–50.

Wang, S.S., Yuan, F.G., 1983. A hybrid finite element approach to composite laminate problems with singularities. J. Appl. Mech. 50, 835–844.

Yamamoto, Y., Sumi, Y., 1978. Stress intensity factors for three-dimensional cracks. Int. J. Fracture 14 (1), 17–38.

Yamamoto, Y., Tokuda, N., 1973. Determination of stress intensity factors in cracked plates by the finite element method. Int. J. Numerical Methods Engng. 6, 427–439.